

Article

# Mitigation of Ice-Induced Vibration of Offshore Platform Based on Gated Recurrent Neural Network

Peng Zhang <sup>1</sup> , Zhihao Wu <sup>1,2</sup>, Chunyi Cui <sup>1,\*</sup> and Ruqing Yao <sup>1</sup>

<sup>1</sup> Department of Civil Engineering, Dalian Maritime University, Dalian 116026, China; peng.zhang47@dmlu.edu.cn (P.Z.); wuzhihao@dmlu.edu.cn (Z.W.); yaoruqing@dmlu.edu.cn (R.Y.)  
<sup>2</sup> Hefei Science and Technology Innovation Group Co., Ltd., Hefei 230000, China  
\* Correspondence: cuichunyi@dmlu.edu.cn

**Abstract:** Ice-induced vibration is one of the major risks that face the offshore platform located in cold regions. In this paper, the gated recurrent neural network (GRNN) is utilized to predict and suppress the response of offshore platforms subjected to ice load. First, a simplified model of the offshore platform is derived and validated based on the finite element model (FEM). The time history of the floating ice load is generated using the harmonic superposition method. Gated Recurrent Unit Network (GRU) and the Long-Short-Term Memory Network (LSTM) are composed in MATLAB to predict the behavior of the off-shore platform. Afterward, the linear quadratic regulator (LQR) control algorithm is used to calculate the controlling force for the training of the GRU/LSTM-based prediction controller. Numerical results show that the ice-induced vibration response prediction method based on GRU network design can predict the structural response with satisfying accuracy, and the ice-induced vibration response control method based on the LSTM network and GRU network design can learn the LQR method well and achieve good control effect. Time lag and other problems that the vibration control programs often encountered were solved well.

**Keywords:** ice-induced vibration; response predict; vibration control; LSTM; GRU



**Citation:** Zhang, P.; Wu, Z.; Cui, C.; Yao, R. Mitigation of Ice-Induced Vibration of Offshore Platform Based on Gated Recurrent Neural Network. *J. Mar. Sci. Eng.* **2022**, *10*, 967. <https://doi.org/10.3390/jmse10070967>

Academic Editor: Barbara Zanuttigh

Received: 24 May 2022

Accepted: 12 July 2022

Published: 14 July 2022

**Publisher's Note:** MDPI stays neutral with regard to jurisdictional claims in published maps and institutional affiliations.



**Copyright:** © 2022 by the authors. Licensee MDPI, Basel, Switzerland. This article is an open access article distributed under the terms and conditions of the Creative Commons Attribution (CC BY) license (<https://creativecommons.org/licenses/by/4.0/>).

## 1. Introduction

Ice-induced vibration is a common threat to offshore platforms. When the floating ice impacts the legs of an offshore platform, a strong motion will be excited at the deck of the platform, resulting in damage to equipment or discomfort of personnel, and some extreme cases causing damage to the platform. Ice-induced vibration was first observed on a jacket offshore platform in Alaska's Cook Inlet in the 1960s [1]. In the Gulf of Bosnia, several lighthouses were damaged by sea ice in the 1970s [2]. In China, the Bohai No.2 platform lost the bearing capacity of the pile leg due to the action of sea ice in 1969, which eventually led to the collapse of the platform and resulted in huge economic losses. In 1977, the Haijin No.4 beacon tower in Bohai Bay was also destroyed due to sea ice. In 2000, serious ice-induced vibration occurred on the JZ20-2MSW platform, causing flange loosening, pipeline rupture, and natural gas leakage [3].

With the accumulation of damage cases caused by floating sea ice, engineers have started to study the hazard mechanism and analysis methods. Szydowski and Kolerski studied the effect of the floating ice on bridge piers using the finite volume method [4]. Istrati et al. studied the tsunami-borne debris loading on coastal bridges using the finite element method [5]. Afterward, Xiang and Istrati [6] proposed an arbitrary Lagrangian–Eulerian method to establish the 3D hydrodynamic model of a deck subjected to extreme wave impacts. The numerical results agreed well with large-scale experimental dataset of a coastal deck. Hasanpour et al. [7] developed a coupled SPH-FEM model to simulate complex turbulent flows and multi-physics interactions across domains (air, fluid, and solid). Abdussamie et al. [8] used the computational fluid dynamic (CFD) approach and the volume of fluid (VOF) to study the wave-in-deck forces on a box-shaped structure. Gotoh

and Khayyer [9] summarized the projection-based particle methods in ocean engineering. Besides, Allsop et al. [10] studied the lateral and uplift forces at the deck of an offshore structure caused by the flow. Xiang et al. [11] proposed a predictive equation to estimate the overturning moment caused by the flow. Afterward, Istrati et al. [12] developed a method to identify the most damaging scenario. The out-of-plane response at the deck and also the yaw and roll moments caused by the impact forces were also investigated [13,14].

Based on the aforementioned studies, a variety of mitigation methods were proposed to reduce the catastrophic damage caused by the floating ice [15]. Currently, methods to reduce the ice-induced vibration of a platform can be divided into two categories. The first category is to install an ice-resistant vertebra to change the action form of ice load and prevent the structure from steady ice-induced vibration. Wang et al. [16,17] verified the effectiveness of the vibration isolation vertebrae in reducing ice-induced vibration response based on the field measured data. Wang et al. [18–20] analyzed the ice-induced vibration characteristics after the installation of ice-resistant vertebrae on the single-pile, four-pile, and multi-pile jacket platform using the method of DEM-FEM. Based on Miner's linear cumulative damage theory and S-N curve, Zhang et al. [21] analyzed the service life and damage of an offshore platform under ice load using ANSYS. The second category is to install dampers to control the vibration response of the structure, which is often divided into passive control, active control, and semi-active control [22,23]. Li et al. [24] studied and verified the effectiveness of the TMD in reducing the ice-induced vibration response of the offshore platform. However, if the frequency of the TMD shifts away from the target frequency of the primary structure, the vibration control effectiveness will be significantly reduced (also known as the detuning effect). To further improve the effectiveness and robustness of the damper, Wu et al. [25] studied the semi-active control algorithm of the MR damper and verified that the MR damper could effectively suppress the vibration of structures under sea ice and seismic loads. Nevertheless, the performance of an MR damper may degrade due to leakage during long-term service. Moreover, Ghadimi et al. [26] conducted a comparative study on the TMD and the semi-active TMD and found that vibration response values of offshore jacket platforms under environmental loads (i.e., wind, water, wave, and sea currents) and seismic loads were significantly reduced.

The recent decade has seen a rapid development of neural networks (NN) and deep learning in both academics and industry, including the field of vibration control. Ma et al. [27] designed a vibration controller based on the BP neural network and realized active vibration control of the offshore platform under the action of random wave force. Cui et al. [28] respectively studied the application of grey prediction, fuzzy neural network, and support vector machine in the field of vibration control of the offshore platform. Chen et al. [29] utilized a multi-layer perceptron and autoregression model to learn the LQR optimal control algorithm and carried out an experimental study to verify its effectiveness. Wang et al. [30] proposed a semi-active non-smooth control algorithm based on deep learning, and the numerical analysis implied that the algorithm had good robustness and anti-interference. Based on the LSTM long-term and short-term neural network, Gao et al. [31,32] studied the structural response prediction and vibration control methods of structures under seismic loads and proved the feasibility of deep neural networks in the field of structural vibration control.

On the basis of previous studies, this paper aims to suppress the ice-induced vibration control of offshore platforms by using a cyclic element network based on gate control. Firstly, the GRU network is proposed to predict the ice-induced vibration response of the offshore jacket platform. According to the predicted response data, the GRU control network and the LSTM control network are constructed, respectively. After training and testing, it is found that both two network control strategies demonstrate a good control effect on the ice-induced vibration of the offshore platform.

## 2. Numerical Model of Offshore Platform and Ice Load

The structure used in this paper is an upright marine jacket structure, designed according to [33,34]. It has two floors and four pile legs. The water depth is 79.5 m, the height of the lower deck is 15.3 m, and the height of the main deck is 23.0 m. The structure above the mud surface is shown in Figure 1 and the structural material properties are listed in Table 1.

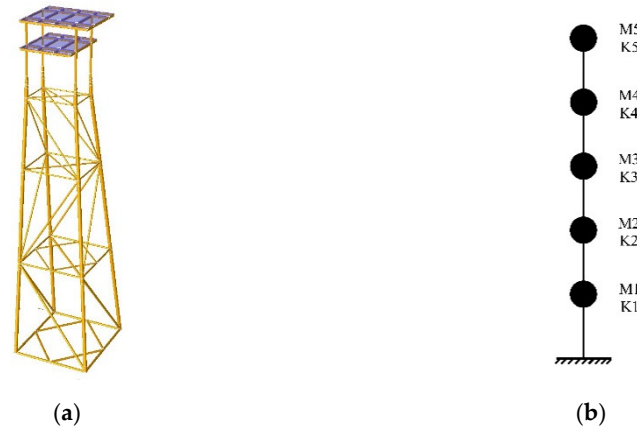


**Figure 1.** Jacket offshore platform model: (a) SACS model of jacket offshore platform; (b) simplified model of jacket offshore platform.

**Table 1.** Structural material properties.

Name of Parameter	Value
E (kN/cm <sup>2</sup> )	20,000
G (kN/cm <sup>2</sup> )	7722
F <sub>y</sub> (kN/cm <sup>2</sup> )	34.5
Density (T/m <sup>3</sup> )	7.849

### 2.1. Simplified Structural Model

Even though the FE model of an offshore platform can predict its dynamic response with high precision, the FE model often contains a large number of degrees of freedom (d.o.f.), which makes it computationally unacceptable for vibration prediction-based control. Consequently, a simplified multi-mass model is established based on the methods proposed by Wang et al. [35].

The structural modal frequency and mode shape are obtained by modal analysis in SACS. These data are input into the model simplification program to obtain the structure parameters of the simplified model. The obtained mass and stiffness are listed in Table 2.

**Table 2.** Structure equivalent parameters and modal values.

Height (m)	Equivalent Stiffness (kg/m)	Equivalent Mass (kg)
−50	$1.433 \times 10^8$	614,190
−21	$7.138 \times 10^8$	421,309
0	$4.432 \times 10^8$	132,653
15.3	$5.567 \times 10^8$	131,660
23	$1.285 \times 10^8$	426,815

To verify the simplified model, the same dynamic load was applied to the SACS model and the simplified model to verify the effectiveness of the simplified model. As shown in Figure 2, the acceleration at the top deck of the platform calculated by the FE model and the simplified model are quite similar, which implies that the accuracy of the simplified model can be accepted.

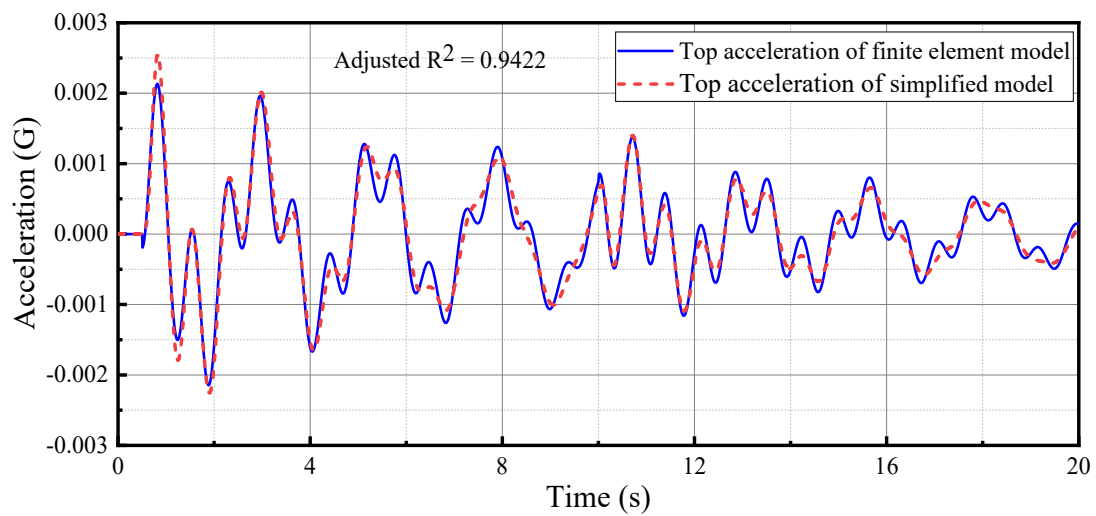


Figure 2. Dynamic response time history curve of jacket offshore platform.

2.2. Ice Load

The ice forces acting on the upright jacket structure without vertebral structure are calculated according to the following formula [33]:

$$F = mIf_c\sigma_cDh \tag{1}$$

where  $m$  is the shape coefficient. For the circular section  $m$  is 0.9, while for the square section  $m$  is 1.0 in the perpendicular direction and 0.7 in the oblique ice direction.  $I$  denotes the embedding coefficient.  $f_c$  is the contact coefficient.  $\sigma_c$  is the unconfined compressive strength of the ice, MPa.  $D$  is the width of the ice extrusion structure, m.  $h$  is ice thickness, m.

The embedding coefficient  $I$  and the contact coefficient  $f_c$  of the pier with a circular section are determined by the following empirical formula [33]:

$$If_c = 3.57h^{0.7} / D^{0.5} \tag{2}$$

where  $h$  is the thickness of ice, cm;  $D$  is the effective diameter of the pile, cm. For circular pier columns with  $2.5 \text{ m} < D < 10 \text{ m}$ ,  $If_c$ : recommended value is generally 0.4; for circular pier columns with  $10 \text{ m} \leq D$ , the recommended  $If_c$  value is generally 0.4~0.25.

The structural dynamic equation of an upright-legged offshore platform under dynamic ice load is as follows:

$$M\ddot{X} + C\dot{X} + KX = F(t) \tag{3}$$

where  $M$  is the structure mass matrix.  $K$  is the structure stiffness matrix.  $C$  is the structural damping matrix.  $F(t)$  is the time-history curve of dynamic ice load.  $X, \dot{X}, \ddot{X}$  are the displacement vector, velocity vector, and acceleration vector, respectively.

When calculating dynamic ice force, the load is usually divided into two parts: fluctuation component and direct flow [36]:

$$F(t) = F_a + F_b(t) \tag{4}$$

where  $F_a$  is the mean value of  $F_b(t)$  and  $F_b(t)$  the fluctuation component of ice load.

The random ice force spectrum and Davenport wind speed spectrum are both low-frequency power spectrums and have similar energy distribution. Methods commonly used to generate time history data include the harmonic superposition method, linear filtering method, wavelet analysis method, etc. In this paper, a simple harmonic superposition method is used to transform the power spectrum of ice load from a frequency domain to a time domain [37].

According to Shinozuka's theory [37], the wave component sample  $F_b$  can be expressed as follows:

$$F_b = F_d(t) = f(n\Delta t) = \sum_{j=1}^M \sqrt{2S_F(\omega_j)\Delta\omega} \cos(\omega_j n\Delta t + \phi_j) \tag{5}$$

where  $S_F$  is the ice load power spectrum of the fluctuating component  $F_b$ ;  $\omega_j$  is the  $J^{\text{th}}$  angular frequency value;  $\Delta\omega$  is angular frequency increment;  $\phi_j$  is a random variable uniformly distributed between 0 and  $2\pi$ ;  $M$  is a sufficiently large spectral density curve equal fraction;  $n$  is the total step of the random process control signal;  $\Delta t$  is the time interval for generating the control signal.

Kärnä et al. [36], based on a large amount of random ice load data measured in Bohai Sea and Bosnia Bay, established the random ice force spectrum after statistical analysis:

$$S(f) = s_F^2 \cdot \frac{1.34v^{-0.6}}{1 + 5v^{-0.9}f^2} \tag{6}$$

$$s_F = \frac{I_F \cdot F_{\max}}{1 + n \cdot I_F} \tag{7}$$

where  $v$  is the ice velocity, m/s.  $f$  is the interval frequency, Hz.  $S_F$  is the standard deviation of maneuvering ice force.  $I_F$  is the action strength of dynamic ice force.  $n$  is a constant, take 3.  $F_{\max}$  is the extreme static ice force, kN.

The average ice load is taken as the direct flow to calculate and the following formula is commonly used:

$$F_a = F_{\text{mean}} = I_F \cdot S_F \tag{8}$$

where  $I_F$  is the strength of moving ice force, generally distributed between 0.2 and 0.6, with an average of 0.4 [36];  $S_F$  is the standard deviation of the ice force with maneuvering.

When calculating the total ice force of a multi-pile offshore platform, the shielding effect of the structure needs to be considered. The vertical leg offshore platform in this paper is a four-leg jacket-type platform without a waterproof casing. According to the direction of sea-ice action, the shielding effect is shown in Figure 3. The effective diameter coefficient of the pile leg affected by the shielding effect is 0.1.

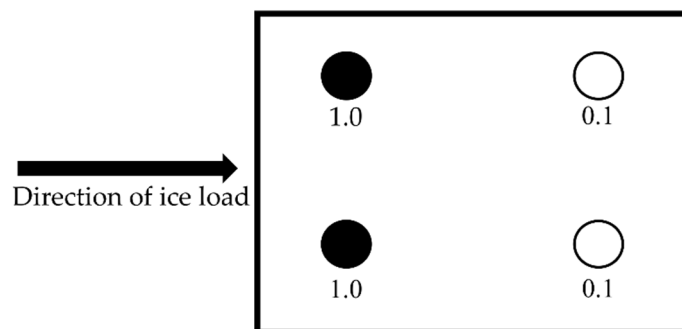


Figure 3. Schematic diagram of shading effect [33].

It should be noted that the hydrodynamic loads will also influence the dynamic response of a structure subjected to wave and floating objects [38–41]. However, this influence is not fully considered in this paper for computation simplicity and efficiency.

### 3. Neural Network Model

Though the artificial neural network (ANN) has been widely accepted in civil engineering for parameter estimation, classification, and pattern recognition, the ANN-based vibration control is relatively less reported. Recently, Sharafati combined the adaptive neuro-fuzzy inference system (ANFIS) with several optimization methods, including particle swarm optimization (PSO), ant colony optimization (ACO), the differential evolution

(DE), and the genetic algorithm (GA) for the prediction of wave-induced scour depth below pipelines. The effectiveness of those methods and their robustness against uncertainties were discussed in detail [42,43]. A stochastic model based on the group method of data handling (GMDH) and the generalized likelihood uncertainty estimation (GLUE) was also proposed. The adequacy and accuracy of the GMDH-GLUE model were validated with numerical results [44].

Traditional control strategies, such as instantaneous optimal control algorithm and pole assignment algorithm, need to obtain the precise model parameters of the structure and that is often difficult to achieve in practical engineering. The neural network control algorithm can adapt to the uncertain model and has good self-learning ability, adaptability, and nonlinear fitting ability. Traditional shallow neural networks, such as Radial Basis Function Network (RBF), have no memory ability and cannot consider the correlation between samples. However, the dynamic response of the structure is time-series data; the state of a specific moment is not only related to the state of the last moment but also related to the state of the past several steps of time.

Recurrent Neural Network (RNN) is a network that has short-term memory capacity. Neurons in this network can receive information not only from themselves but also from other neurons. RNN is often used in temporal problems such as speech recognition and natural language generation. Based on RNN, the Long Short-Term Memory Network (LSTM) proposed by Hochreiter and Schmidhuber et al. [45] and the Gated Recurrent Unit Network (GRU) proposed by Cho et al. [46,47] and Chung et al. [48] are the most widely used recurrent neural networks. This kind of network can effectively solve the problem of gradient disappearance or explosion frequently encountered in the RNN network by introducing a gating unit.

### 3.1. Basis of LSTM and GRU

In the LSTM, there are three control units called gates: input gate ( $i_t$ ), output gate ( $o_t$ ), and forget Gate ( $f_t$ ). The input gate determines how much information from the current state of the network needs to be stored in the internal state, and then the forgetting gate determines how much information from the past state needs to be discarded. Besides, the output gate determines how much information about the current internal state needs to be output to the external state. The output gate is achieved by introducing a logistic function,  $\sigma$ , a function whose output is distributed between 0 and 1, indicating that information is allowed to pass in a certain proportion.

The calculation process of LSTM is as follows: firstly, the external state  $h_t$  at the last moment and the input  $x_t$  at the current moment are used to calculate the values of the three gates ( $i_t, o_t, f_t$ ) and candidate states  $\tilde{c}_t$ . Then combining the forgetting gate  $f_t$  and the input gate  $i_t$  updates the memory unit  $c_t$ . Finally, the internal information is transmitted to the external state  $h_t$  according to the output gate  $o_t$ . This process can be expressed as follows:

$$\begin{bmatrix} \tilde{c}_t \\ o_t \\ i_t \\ f_t \end{bmatrix} = \begin{bmatrix} \tanh \\ \sigma \\ \sigma \\ \sigma \end{bmatrix} (W \begin{bmatrix} x_t \\ h_{t-1} \end{bmatrix} + b) \tag{9}$$

$$c_t = f_t \odot c_{t-1} + i_t \odot \tilde{c}_t \tag{10}$$

$$h_t = o_t \odot \tan h(c_t) \tag{11}$$

where  $x_t \in R^M$  is the input data at the current moment  $W \in R^{4D \times (D+M)}$  and  $b \in R^{4D}$  are parameters of the network.

Compared with the LSTM, the network structure of the GRU is simpler. Different from the LSTM, the GRU combines the input gate and the forget gate into one gate, which is called the update gate. In the GRU, there is no division of internal state and external state in a network, and a linear dependency relationship is directly added between the current network state  $h_t$  and the last network state  $h_{t-1}$  to solve the problem of gradient

disappearance and gradient explosion. The calculation formula for updating gate  $z_t$  and resetting gate  $r_t$  in GRU is as follows:

$$\text{Updating gate : } z_t = \sigma(W_z x_t + U_z h_{t-1} + b_z) \quad (12)$$

$$\text{Resetting gate : } r_t = \sigma(W_r x_t + U_r h_{t-1} + b_r) \quad (13)$$

$$\text{Output : } h_t = z_t \odot h_{t-1} + (1 - z_t) \odot \tilde{h}_t \quad (14)$$

where  $x_t$  is the input data at the current moment,  $W_z$ ,  $W_r$ ,  $U_z$ ,  $U_r$ ,  $b_z$ , and  $b_r$  correspond to the weight matrix and coefficient vector of the updated gate and reset gate, respectively.

When  $z_t = 0$ ,  $r = 1$ , the GRU degenerates into a simple cyclic network. When  $z_t = 0$ ,  $r = 0$ , the current state  $h_t$  is only related to the current input  $x_t$ , and has nothing to do with the historical state  $h_t$ . When  $z_t = 1$ , the current state  $h_t$  is equal to the previous state  $h_{t-1}$ , which is independent of the current input  $x_t$ . Unlike the LSTM, the GRU has no separate storage unit, so the operation cost is lower, and the data learning ability is not as good as the LSTM.

Overfitting is a common problem in machine learning due to the limited training data and the network structure. In a previous study, Srivastava et al. [49] proposed to add a Dropout layer to eliminate overfitting and enhance the model robustness. The principle of Dropout regularization is to make the neurons in the neural network randomly inactivate at the appropriate scale so that the model does not become overly dependent on a particular neuron.

The standardization of data is to scale the data in proportion and make it fall into a small specific interval, which makes the calculation of loss function simpler and faster. The commonly used normalization methods include scaling normalization and Z-score normalization. In this paper, the Z-Score normalization is used since the response data generated by structural vibration has a strong disorder and no obvious boundary. The mean value  $\mu$  and standard deviation  $\sigma$  of the data were calculated, and the normalized data with normal distribution was obtained by Gaussian mapping.

### 3.2. Forecast Network Model

In a structural vibration control program, the time lag is inevitable due to various reasons. In this paper, a gating-based cyclic neural network prediction method is proposed to forecast the structural response. This method can predict the response of the next time step based on the monitored structural response of several previous steps. Then the predicted response will be transmitted to a controller to calculate the controlling force of the next step. In this way, the time lag can be addressed. The LSTM and the GRU can be built by the MATLAB deep learning toolbox and the prediction effect of these two commonly used cyclic networks on structural ice-induced vibration response will be discussed.

The structural parameters and training hyperparameters of the LSTM and the GRU will be determined after several rounds of trial calculation. As shown in Figure 4, the LSTM is a deep network with five layers (the input layer, the LSTM layer, the dropout layer, the full connection layer, and the output layer). The LSTM layer is a recursive loop layer containing 128 gating units and the random loss rate of the dropout layer is 0.5. As a forecast network model, the GRU has similar parameters to the LSTM (just change the LSTM layer to the GRU layer). For the training hyperparameter, the Adam optimizer was used for both networks, the initial learning rate was set as 0.005 and the number of training was set as 100.

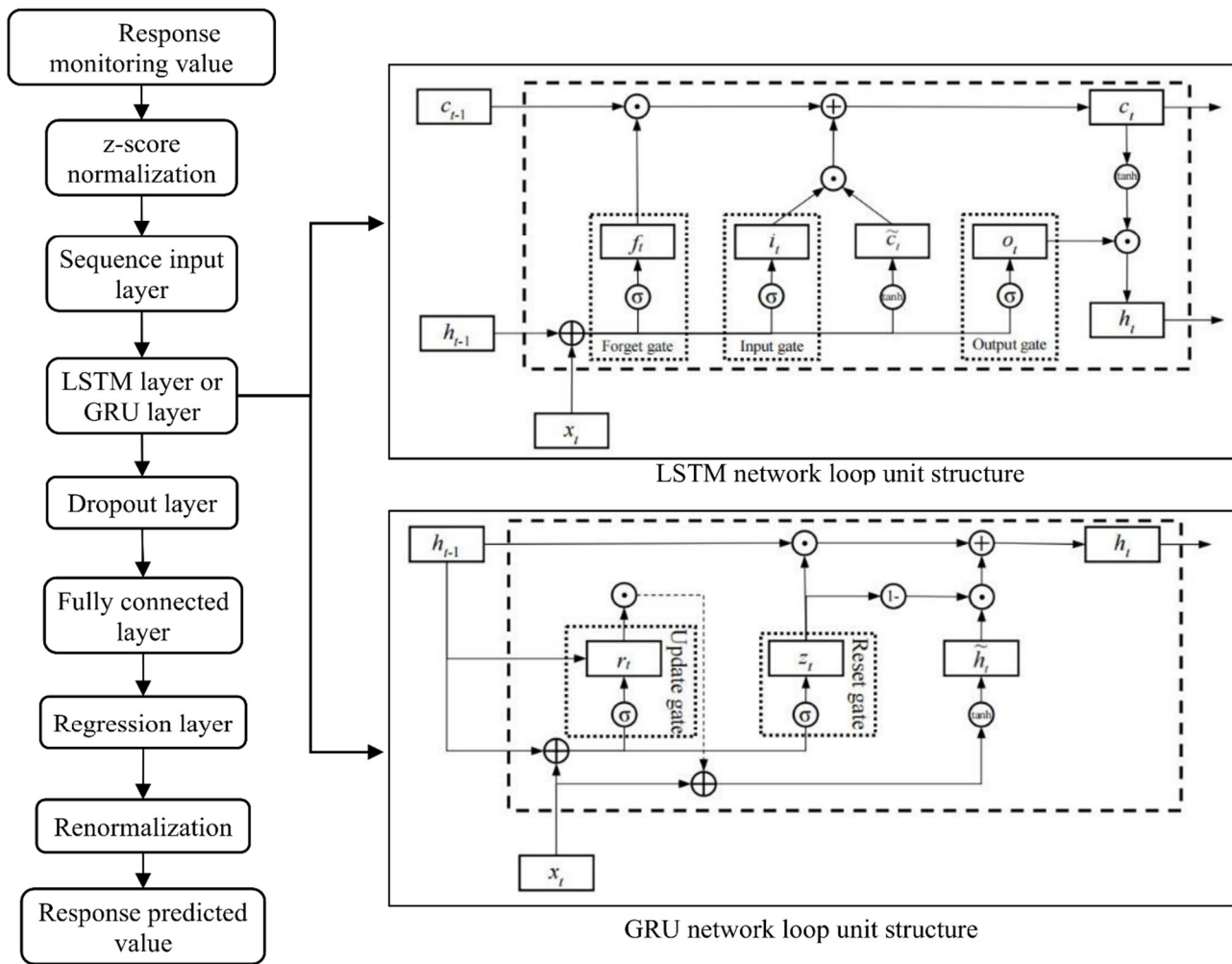


Figure 4. Predictive network structure diagram.

### 3.3. Control Network Model

The LQR algorithm has high requirements for the accuracy of the structural model and poor generalization for different external excitations, which limits its application in a real-world project. However, the controlling force calculated by the LQR method can be used to train the neural network-based vibration controller [32]. The predicted response of the offshore platform and the ice load is the input of the neural network, while the output is the controlling force. The load value, response value, and corresponding control force under different ice conditions are used as training set and verification set, respectively, to verify that the control system has good generalization performance.

According to experience, there will be four feature combinations discussed in this paper and they are displacement and load value, velocity and load value, acceleration and load value, and displacement, velocity, acceleration, and load value, respectively. In addition, the data of the ice-induced vibration response by predicting as the input data will verify the feasibility of the prediction data in the control program to calculate the control force.

The network structure is shown in Figure 5. By empirical calculation, the network with a single structural response and load as input data is a 4-layer network: input layer, LSTM layer (GRU layer), full-connection layer, and output layer. The gated cyclic layer contains 128 gated units and the initial learning rate is set at 0.005 and 100 times of training. If the input data is a combination of displacement, velocity, acceleration, and load values, the network structure will have five layers, a dropout layer with a random loss rate of 0.5 should be added after the gated loop layer to prevent data overfitting.

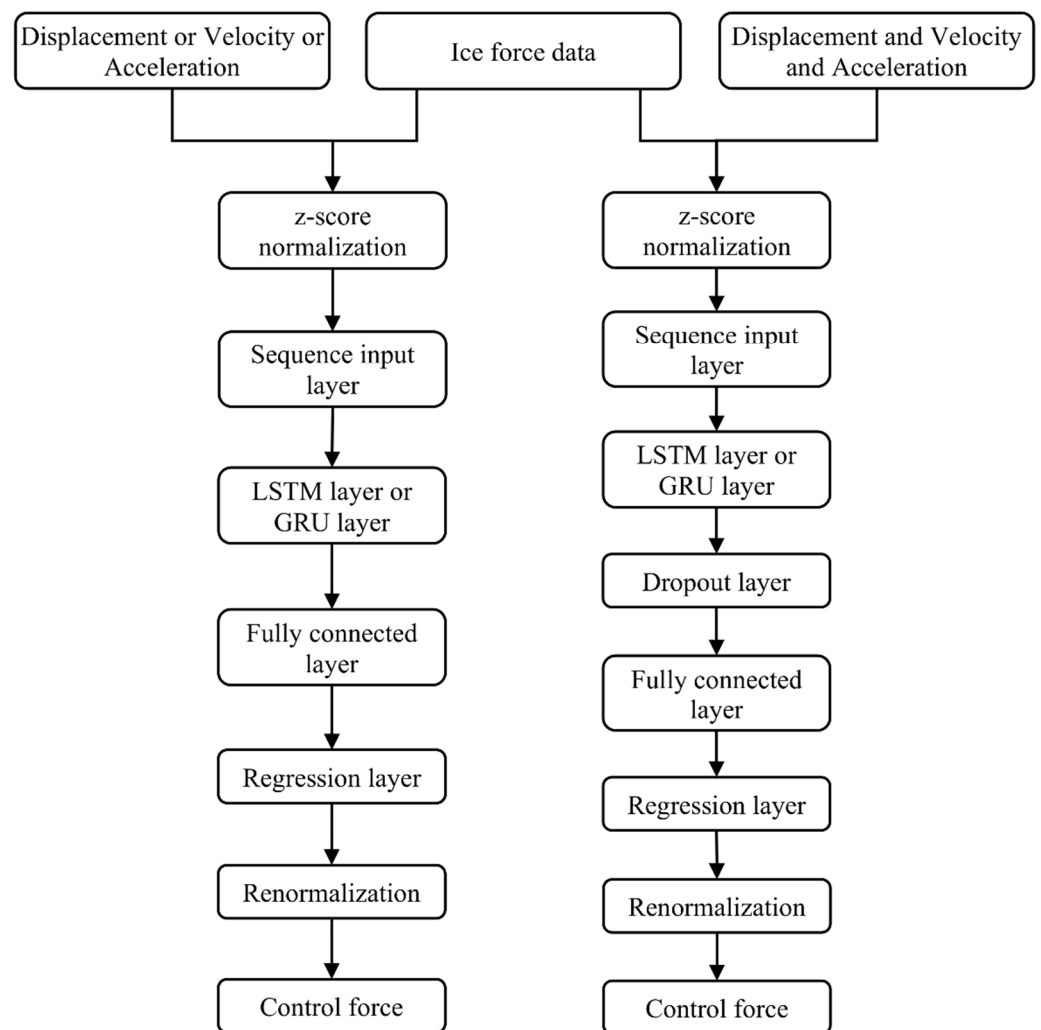


Figure 5. Control program network structure.

Through several rounds of trial and optimization, the structure of the network is determined. The network is composed of 4 layers: the input layer, the LSTM layer (or the GRU layer), the full-connection layer, and the output layer. The layer of the gated cyclic layer contains 128 gated units and the initial learning rate is set at 0.005 and 1000 times of training. Other network parameters and training parameters remain unchanged and Adam optimizer is used for network training.

#### 4. Network Model Analysis

##### 4.1. Structural Analysis of Forecast Network

The simplified model of the offshore jacket platform is used to calculate the ice-induced vibration dynamic response of the structure, and the result is used as the data set for training and validation of the networks. The LSTM and the GRU are built by MATLAB deep learning toolbox, and the prediction effects of these two commonly used cyclic networks on structural ice-induced vibration are discussed.

The ice-induced vibration responses of the structure under different ice conditions were calculated by the MATLAB program, and the numerical results will be separated as training set and test set, respectively. The data of displacement, velocity, and acceleration that at time T will be used as input data and that at time T + 11 will be regarded as output time. The ice-induced vibration response of the offshore platform under the ice speed of 0.9 m/s, ice thickness of 0.6 m, and ice strength of 1.8 MPa was used as the training set.

The Adjusted  $R^2$  (adjusted determination coefficient) is defined as follows to compare the performance of the GRU and the LSTM network:

$$R_{adjusted} = 1 - \frac{(1 - R^2)(n - 1)}{n - p - 1} \tag{15}$$

where  $n$  is the number of the samples, and  $p$  is the number of the predicted variables. In this paper, the two neural networks were used to predict the response of displacement, velocity, and acceleration, then  $p$  is set to 3.  $R^2$  is defined as follows:

$$R^2 = 1 - \frac{\sum (Y_{actual} - Y_{predict})^2}{\sum (Y_{actual} - Y_{mean})^2} \tag{16}$$

in which  $Y_{actual}$  and  $Y_{predict}$  are the real response and the predicted response, respectively.

As shown in Table 3, although the Adjusted  $R^2$  of the speed predicted by the GRU and the LSTM is not significantly different, the Adjusted  $R^2$  of the displacement predicted value and the acceleration predicted values are significantly different. The minimum Adjusted  $R^2$  of the GRU displacement prediction value was 0.9833, and the minimum Adjusted  $R^2$  of the LSTM displacement prediction value was 0.9283. The minimum Adjusted  $R^2$  of the GRU acceleration prediction value was 0.9286, and the minimum Adjusted  $R^2$  of the LSTM acceleration prediction value was 0.8995. Therefore, the prediction effect of the GRU is significantly better than that of the LSTM. In addition, the internal structure of the GRU is simpler than the LSTM, so the speed of training and operation is faster. Therefore, the GRU will be used to predict the structural dynamic response of ice-induced vibration.

**Table 3.** Structural response prediction analysis table.

Network Type	Ice Conditions	Adjusted $R^2$		
		Displacement	Velocity	Acceleration
GRU Network	$V = 0.8 \text{ m/s}, H = 0.4 \text{ m}, \sigma = 2.2 \text{ MPa}$	0.9929	0.9685	0.9322
	$V = 1.0 \text{ m/s}, H = 0.5 \text{ m}, \sigma = 2.0 \text{ MPa}$	0.9925	0.9725	0.9286
	$V = 1.0 \text{ m/s}, H = 0.46 \text{ m}, \sigma = 1.6 \text{ MPa}$	0.9833	0.9698	0.9322
LSTM Network	$V = 0.8 \text{ m/s}, H = 0.4 \text{ m}, \sigma = 2.2 \text{ MPa}$	0.9814	0.9652	0.9036
	$V = 1.0 \text{ m/s}, H = 0.5 \text{ m}, \sigma = 2.0 \text{ MPa}$	0.9888	0.9710	0.8995
	$V = 1.0 \text{ m/s}, H = 0.46 \text{ m}, \sigma = 1.6 \text{ MPa}$	0.9283	0.9679	0.9056

#### 4.2. Analysis of Computing Structure of Control Network

Two hundred groups of experiments were carried out for different input methods of the GRU and the LSTM, respectively. The modified determination coefficient of each operation result was calculated as well as its maximum value, minimum value, average value, and standard deviation were counted. The research results are shown in Table 4. When a single response characteristic is input data, the maximum correction coefficient of control force calculated by the GRU is 0.891 and the maximum correction coefficient of control force calculated by the LSTM is 0.969. When combined input of response characteristics is used, the maximum correction coefficients of control force calculated by the GRU and the LSTM are 0.986 and 0.983, respectively. It can be found that the control force calculated by combined input is significantly better than that calculated by single response input. And the standard deviation of the combined input is far less than that of the single input, which proves that the network stability is better when the combined input is used.

**Table 4.** Control network calculation analysis table.

	GRU				LSTM			
	Input 1	Input 2	Input 3	Input 4	Input 1	Input 2	Input 3	Input 4
MAX	0.868	0.891	0.857	0.986	0.969	0.897	0.911	0.983
MIN	0.397	0.501	−0.721	0.942	0.784	0.588	0.508	0.928
AVG	0.778	0.772	0.443	0.972	0.935	0.829	0.815	0.964
S.D.	0.080	0.071	0.237	0.009	0.026	0.042	0.067	0.010

**5. Case Study**

*5.1. Prediction of Structural Ice-Induced Vibration Response*

According to relevant specifications, the forecast of ice-induced vibration response of a jacket platform is analyzed when the strength of sea ice is 2.2 MPa, the thickness of ice is 40 cm and the ice speed is 0.8 m/s. The simplified model is used to calculate in the MATLAB program. First, the prediction of the GRU network will be verified that it is effective. As shown in Figure 6, the Adjusted  $R^2$  of the predicted value of displacement response was 0.9987, the Adjusted  $R^2$  of the predicted value of speed response was 0.9685, and the Adjusted  $R^2$  of the predicted value of speed response was 0.9322. It is proven that the GRU is effective at predicting ice vibration response.

*5.2. Control of The Ice-Induced Vibration*

As shown in Figure 7, the LSTM control method and GRU control method proposed based on the GRU predicted response data have a good vibration control ability after learning the LQR optimal control algorithm. The control effect is shown in the following Table 5.

As shown in Table 5, the LSTM control method and GRU control algorithm proposed based on the GRU predicted response data have good vibration control ability after learning the LQR optimal control algorithm. Among them, the structure uncontrolled displacement peak is 4.20 cm, the LSTM algorithm is used to reduce to 3.34 cm, decreased 20.42%, the GRU algorithm is used to reduce to 3.44 cm, decreased 18.21%, the LQR algorithm is used to reduce to 3.30 cm, decreased 21.24%; the structure uncontrolled speed peak is 7.53 m/s, the LSTM algorithm is used to reduce to 5.23 cm/s, decreased 30.58%, the GRU algorithm is used to reduce to 5.30 cm/s, decreased 29.66%, the LQR algorithm is used to reduce to 5.36 cm/s, decreased 28.79%; the structure uncontrolled acceleration peak is 26.81 cm/s<sup>2</sup>, LSTM algorithm is used to reduce to 17.02 cm/s<sup>2</sup>, decreased 36.54%, the GRU algorithm is used to reduce to 17.71 cm/s<sup>2</sup>, decreased 33.96%, the LQR algorithm is used to reduce to 18.13 cm/s<sup>2</sup>, decreased 32.40%.

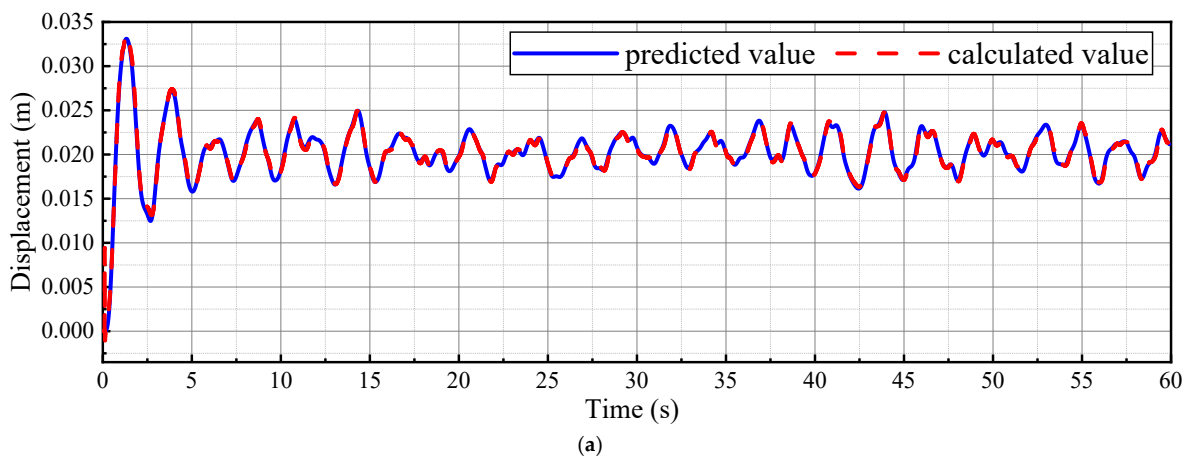


**Figure 6.** Cont.

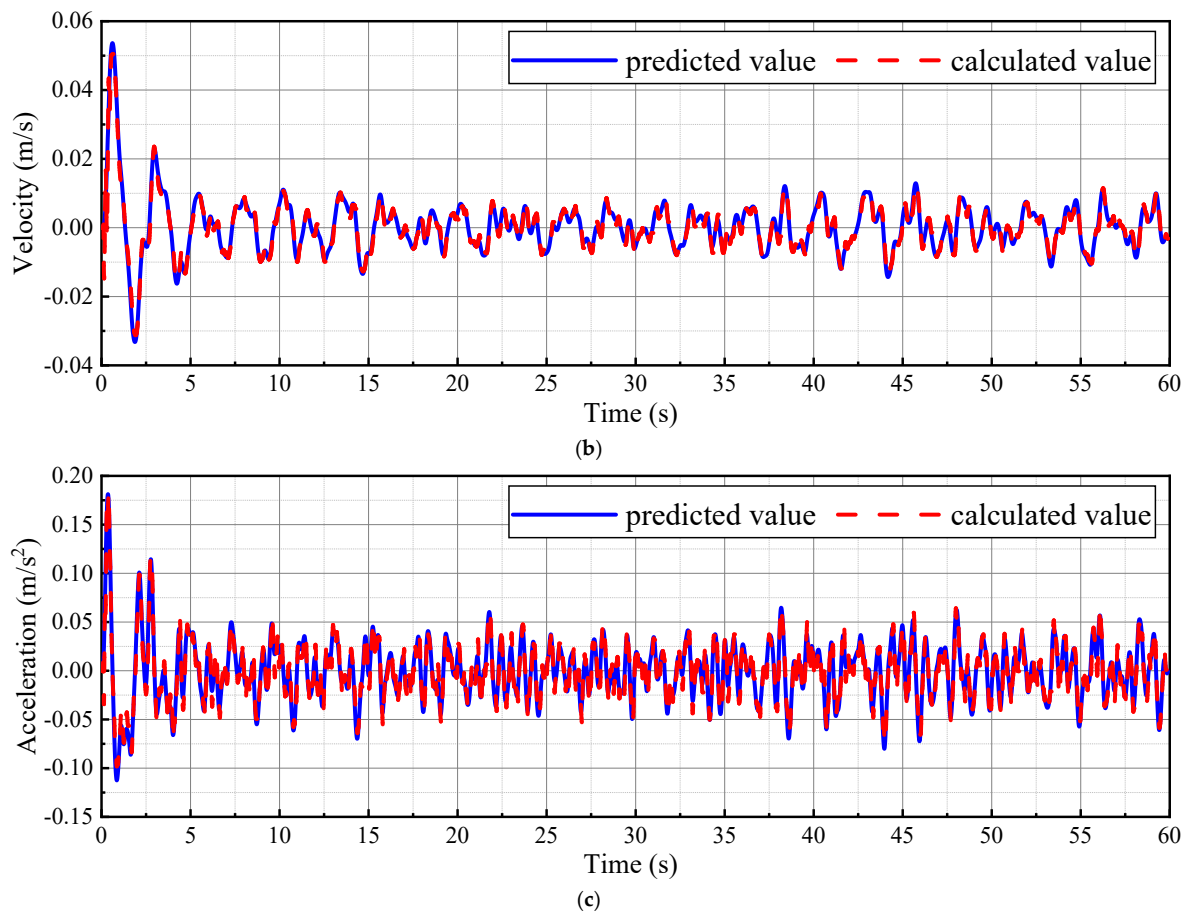


**Figure 6.** Ice-induced vibration response prediction of jacket offshore platform: (a) prediction of ice-induced vibration displacement of jacket offshore platform; (b) velocity response prediction of ice-induced vibration of jacket offshore platform; (c) acceleration response prediction of ice-induced vibration of jacket offshore platform.

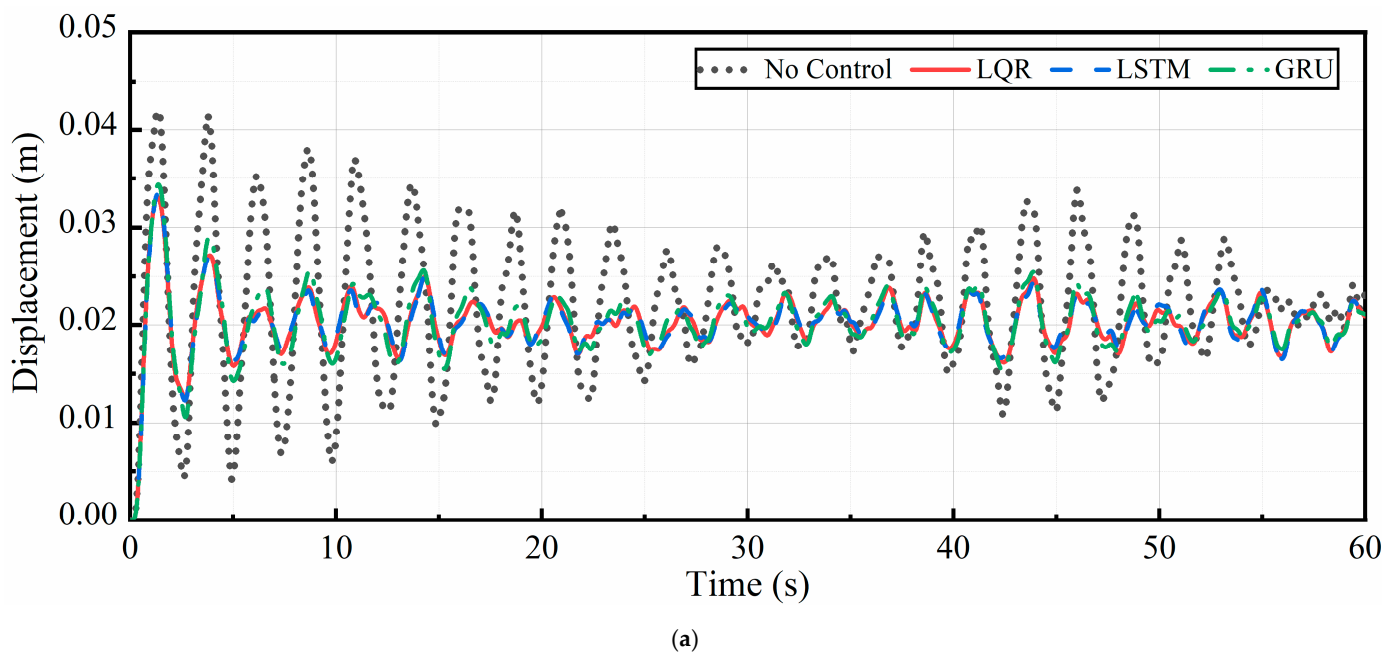
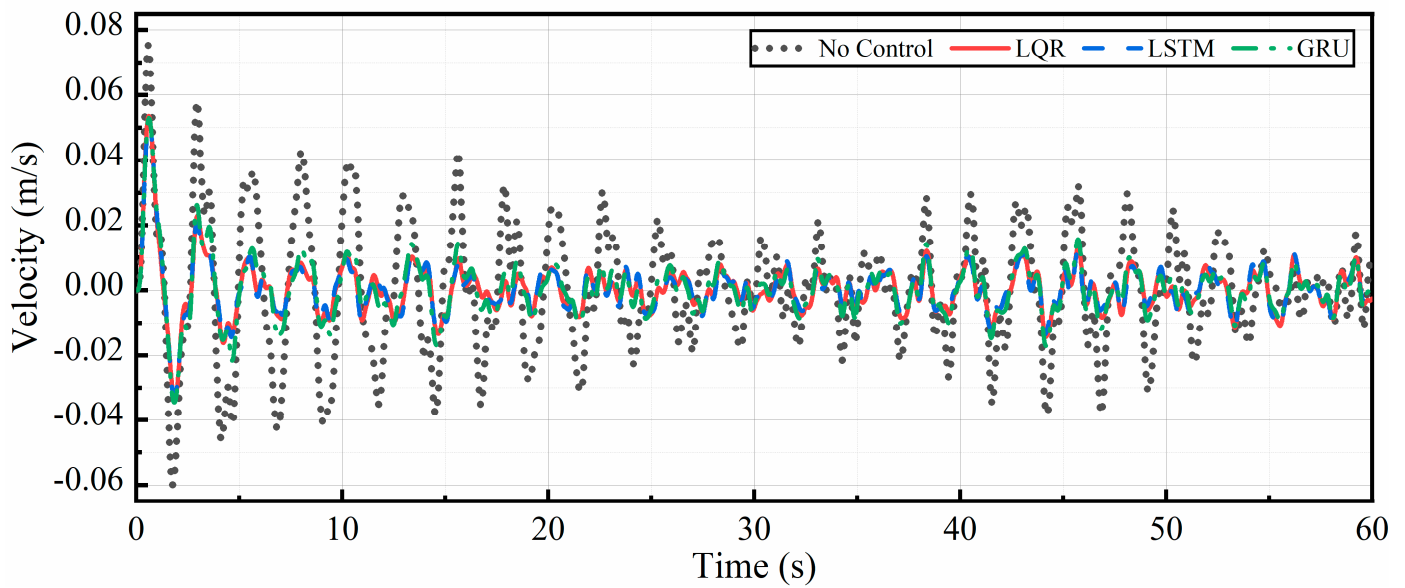
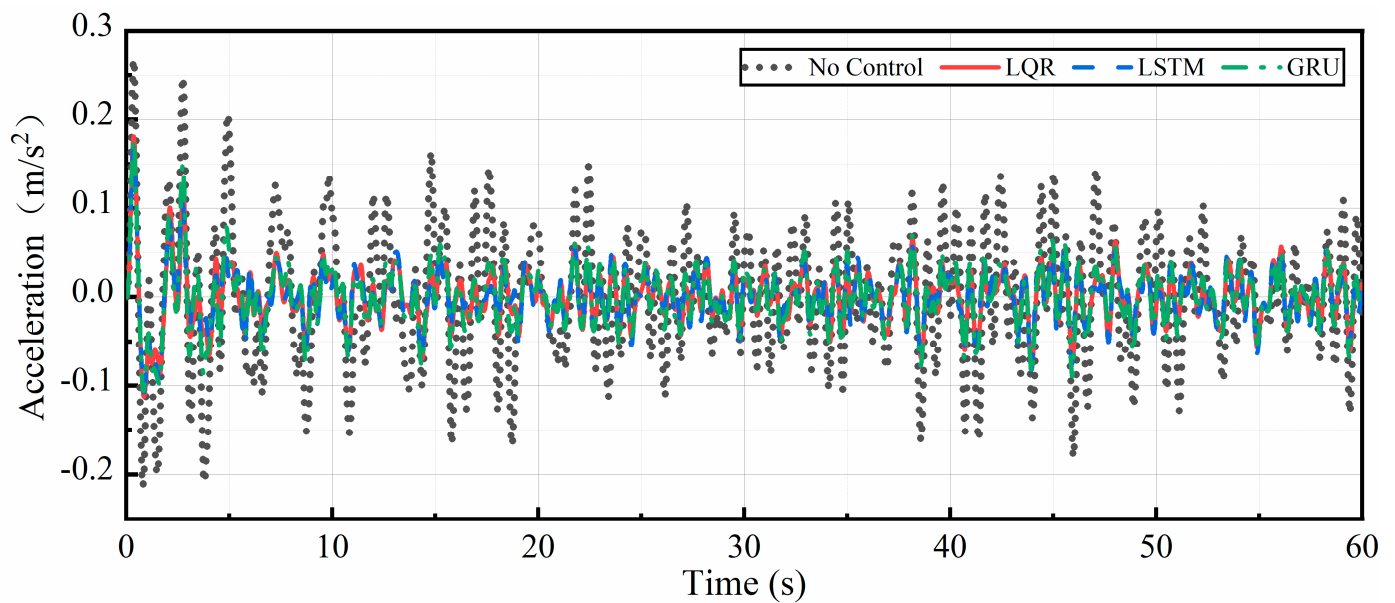


**Figure 7.** Cont.



(b)



(c)

Figure 7. Top response time history curve: (a) displacement response time history curve; (b) velocity response time history curve; (c) acceleration response time history curve.

Table 5. Response control analysis table.

Control Strategy	Displacement (cm)		Velocity (cm/s)		Acceleration (cm/s <sup>2</sup> )	
	Peak	Drop	Peak	Drop	Peak	Drop
Without control	4.20	-	7.53	-	26.81	-
LQR	3.30	21.24%	5.36	28.79%	18.13	32.40%
GRU	3.44	18.21%	5.30	29.66%	17.71	33.96%
LSTM	3.34	20.42%	5.23	30.58%	17.02	36.54%

## 6. Conclusions

Based on the gated cycle neural network, this paper studies the ice-induced vibration response control method of the offshore jacket platform. The major findings are as follows:

- (1) Based on the structural modal parameters, the structural parameters of the simplified model were identified. According to the verification results of its dynamic response, it is proved that the simplified model can well reflect the dynamic response characteristics of the original finite-element model.
- (2) A prediction model of ice-induced vibration response based on the GRU neural network is proposed, which can effectively predict the future structural response according to the current structural response of the platform, and is applied to the vibration control program to solve the problem of the control program time lag.
- (3) It is found that the LSTM and the GRU both can learn LQR optimal control algorithm well and have a good control effect for different working conditions, indicating that the LSTM has good robustness. The response control effect of the LSTM control strategy is slightly better than that of the GRU under the condition of sacrificing a certain calculation time.

Moreover, the ice load considered in this study is simplified for computational efficiency, with the hydrodynamic effect ignored. Besides, the ice load is only applied at a specific height of the leg as a point load. Ice load applied to the deck of the platform may also cause serious damage. In the future, a more sophisticated ice force model shall be considered and the ice load shall be applied to different nodes of the offshore platform from different angles to investigate the robustness of the LSTM and the GRU-based controller.

**Author Contributions:** Conceptualization, P.Z. and Z.W.; methodology, P.Z. and Z.W.; software, Z.W.; validation, C.C., Z.W. and P.Z.; formal analysis, P.Z.; investigation, Z.W. and R.Y.; resources, P.Z.; data curation, Z.W.; writing—original draft preparation, Z.W. and P.Z.; writing—review and editing, P.Z., R.Y. and C.C.; visualization, Z.W. and R.Y.; supervision, C.C.; project administration, C.C.; funding acquisition, P.Z. All authors have read and agreed to the published version of the manuscript.

**Funding:** This research was funded by the National Natural Science Foundation of China (NSFC), grant number 51808092; United Navigation Foundation of Liaoning Province, grant number 2020-HYLH-48; the National Key R&D Program of China (2021YFB2601102); and the open fund of State Key Laboratory of Coastal and Offshore Engineering (DUT-LP2122).

**Institutional Review Board Statement:** Not applicable.

**Informed Consent Statement:** Not applicable.

**Data Availability Statement:** The data used to support the findings of this study are available from the corresponding author upon request.

**Conflicts of Interest:** The authors declare no conflict of interest.

## References

1. Sinha, N.K.; Timco, G.W.; Frederking, R. Recent Advances in Ice Mechanics in Canada. *Appl. Mech. Rev.* **1987**, *40*, 1214–1231. [[CrossRef](#)]
2. Engelbrekton, A.; Janson, J.E. Field Observations of Ice Action on Concrete Structures in the Baltic Sea. *Concr. Int.* **1985**, *7*, 48–52.
3. Zhang, D.; Yu, S.; Wang, Y.; Yue, Q. Sea Ice Management for Oil and Gas Platforms in the Bohai Sea. *Pol. Marit. Res.* **2017**, *24*, 195–204. [[CrossRef](#)]
4. Szydłowski, M.; Kolerski, T. Numerical modeling of water and ice dynamics for analysis of flow around the Kiezmark Bridge piers. In *Free Surface Flows and Transport Processes*; Springer: Berlin/Heidelberg, Germany, 2018; pp. 465–476.
5. Istrati, D.; Hasanpour, A.; Buckle, I. Numerical investigation of tsunami-borne debris damming loads on a coastal bridge. In *Proceedings of the 17 World Conference on Earthquake Engineering, Sendai, Japan, 13–18 September 2020*.
6. Xiang, T.; Istrati, D. Assessment of Extreme Wave Impact on Coastal Decks with Different Geometries via the Arbitrary Lagrangian-Eulerian Method. *J. Mar. Sci. Eng.* **2021**, *9*, 1342. [[CrossRef](#)]
7. Hasanpour, A.; Istrati, D.; Buckle, I. Coupled SPH-FEM Modeling of Tsunami-Borne Large Debris Flow and Impact on Coastal Structures. *J. Mar. Sci. Eng.* **2021**, *9*, 1068. [[CrossRef](#)]

8. Abdussamie, N.; Thomas, G.; Amin, W.; Ojeda, R. Wave-in-deck forces on fixed horizontal decks of offshore platforms. In Proceedings of the International Conference on Offshore Mechanics and Arctic Engineering, San Francisco, CA, USA, 8–13 June 2014; American Society of Mechanical Engineers: New York, NY, USA, 2014; p. V1A.
9. Gotoh, H.; Khayyer, A. Current achievements and future perspectives for projection-based particle methods with applications in ocean engineering. *J. Ocean. Eng. Mar. Energy* **2016**, *2*, 251–278. [[CrossRef](#)]
10. Allsop, W.; Cuomo, G.; Tirindelli, M. New prediction method for wave-in-deck loads on exposed piers/jetties/bridges. In Proceedings of the Coastal Engineering 2006—30th International Conference, San Diego, CA, USA, 3–8 September 2006; Volume 5, pp. 4482–4493.
11. Xiang, T.; Istrati, D.; Yim, S.C.; Buckle, I.G.; Lomonaco, P. Tsunami loads on a representative coastal bridge deck: Experimental study and validation of design equations. *J. Waterw. Port. Coast. Ocean. Eng.* **2020**, *146*, 4020022. [[CrossRef](#)]
12. Istrati, D.; Buckle, I.; Lomonaco, P.; Yim, S. Deciphering the Tsunami Wave Impact and Associated Connection Forces in Open-Girder Coastal Bridges. *J. Mar. Sci. Eng.* **2018**, *6*, 148. [[CrossRef](#)]
13. Istrati, D.; Buckle, I.G. *Tsunami Loads on Straight and Skewed Bridges—Part 1: Experimental Investigation and Design Recommendations*; Department of Transportation, Research Section: Salem, OR, USA, 2021.
14. Istrati, D.; Buckle, I.G. *Tsunami Loads on Straight and Skewed Bridges—Part 2: Numerical Investigation and Design Recommendations*; Department of Transportation, Research Section: Salem, OR, USA, 2021.
15. Zhang, D.; Xu, N.; Yue, Q.; Liu, D. Sea Ice Problems in Bohai Bay Oil and Gas Exploitation. *J. Coast. Res.* **2015**, *73*, 676–680. [[CrossRef](#)]
16. Wang, S.; Yue, Q. Vibration Reduction of Bucket Foundation Platform with Fixed Ice-Breaking Cone in the Bohai Sea. *J. Cold Reg. Eng.* **2012**, *26*, 160–168. [[CrossRef](#)]
17. Wang, S.; Yue, Q. Ice induced vibration and its isolation of an offshore platform with bucket foundations in marginal oilfields. In Proceedings of the 29th International Conference on Ocean, Offshore and Arctic Engineering, Shanghai, China, 6–11 June 2010; ASME: Houston, TX, USA, 2010; Volume 4.
18. Ji, S.; Wang, S. A Coupled Discrete–Finite Element Method for the Ice-Induced Vibrations of a Conical Jacket Platform with a GPU-Based Parallel Algorithm. *Int. J. Comput. Methods* **2019**, *17*, 1850147. [[CrossRef](#)]
19. Wang, S.; Ji, S. DEM-FEM modelling interaction between level ice and conical jacket platform. In Proceedings of the 24th International Conference on Port and Ocean Engineering under Arctic Conditions, Busan, Korea, 11–16 June 2017.
20. Wang, S.; Ji, S. Ice induced vibration of conical platform based on coupled DEM-FEM model with high efficiency algorithm. *Haiyang Xuebao* **2017**, *39*, 98–107.
21. Zhang, D.; Wang, G.; Yue, Q. Evaluation of Ice-Induced Fatigue Life for a Vertical Offshore Structure in the Bohai Sea. *Cold Reg. Sci. Technol.* **2018**, *154*, 103–110. [[CrossRef](#)]
22. Zhang, B.-L.; Han, Q.-L.; Zhang, X.-M. Recent Advances in Vibration Control of Offshore Platforms. *Nonlinear Dyn.* **2017**, *89*, 755–771. [[CrossRef](#)]
23. Kandasamy, R.; Cui, F.; Townsend, N.; Foo, C.C.; Guo, J.; Sheno, A.; Xiong, Y. A Review of Vibration Control Methods for Marine Offshore Structures. *Ocean. Eng.* **2016**, *127*, 279–297. [[CrossRef](#)]
24. Li, D.; Zhang, D.; Yue, Q. Phase analysis on the mechanism of TMD and mitigation of ice-induced vibrations for jacket platforms with TMD. In Proceedings of the 29th International Conference on Ocean, Offshore and Arctic Engineering, Shanghai, China, 6–11 June 2010; Volume 49125, pp. 837–845.
25. Wu, B.; Shi, P.; Wang, Q.; Guan, X.; Ou, J. Performance of an Offshore Platform with MR Dampers Subjected to Ice and Earthquake. *Struct. Control. Health Monit.* **2010**, *18*, 682–697. [[CrossRef](#)]
26. Ghadimi, B.; Taghikhany, T. Dynamic Response Assessment of an Offshore Jacket Platform with Semi-Active Fuzzy-Based Controller: A Case Study. *Ocean. Eng.* **2021**, *238*, 109747. [[CrossRef](#)]
27. Ma, H.; Zhang, Y.; Tang, G.-Y.; Zhang, B.-L. BP Neural network vibration control with time delay for offshore platforms under wave forces. In Proceedings of the 2017 36th Chinese Control Conference (CCC), Dalian, China, 26–28 July 2017.
28. Cui, H.; Hong, M. Adaptive inverse control of offshore jacket platform based on grey prediction. In Proceedings of the 2011 Second International Conference on Digital Manufacturing; Automation, Zhangjiajie, China, 5–7 August 2011.
29. Chen, P.-C.; Chien, K.-Y. Machine-Learning Based Optimal Seismic Control of Structure with Active Mass Damper. *Appl. Sci.* **2020**, *10*, 5342. [[CrossRef](#)]
30. Wang, Q.; Wang, J.; Huang, X.; Zhang, L. Semiactive Nonsmooth Control for Building Structure with Deep Learning. *Complexity* **2017**, *2017*, 1–8. [[CrossRef](#)]
31. Gao, J.; Zhang, C. Structural Seismic Response Prediction Based on Long Short-Term Memory Network. *Earthq. Resist. Eng. Retrofit.* **2020**, *42*, 130–134. [[CrossRef](#)]
32. Tu, J.; Gao, J.; Li, Z.; Zhang, J. Research on Structural Intelligent Control Algorithms Based on Long Short-Term Memory Networks. *J. Huazhong Univ. Sci. Tech. (Nat. Sci. Ed.)* **2019**, *47*, 110–115. [[CrossRef](#)]
33. China Nation Offshore Oil Corporation. *Provisions for Sea Ice Conditions and Applications in the China Sea*; China Nation Offshore Oil Corporation: Tianjin, China, 2002.
34. China Classification Society. *Guide for Analysis of Ice-induced Vibration and Ice-induced Fatigue of Stationary Marine Steel Structures*; China Classification Society: Beijing, China, 2018.

35. Wang, S.; Li, H.; Ji, C.; Jiao, G. Energy Analysis for TMD-Structure Systems Subjected to Impact Loading. *Chain. Ocean. Eng.* **2002**, *16*, 301–310.
36. Kärnä, T.; Qu, Y.; Ku Hnlein, W.L. A New spectral method for modeling dynamic ice actions. In Proceedings of the 23rd International Conference on Offshore Mechanics and Arctic Engineering, Vancouver, BC, Canada, 20–25 June 2004; pp. 953–960.
37. Shinozuka, M.; Jan, C.-M. Digital Simulation of Random Processes and Its Applications. *J. Sound Vib.* **1972**, *25*, 111–128. [[CrossRef](#)]
38. Anagnostopoulos, S.A. Dynamic response of offshore platforms to extreme waves including fluid-structure interaction. *Eng. Struct.* **1982**, *4*, 179–185. [[CrossRef](#)]
39. Istrati, D.; Buckle, I.G. Effect of fluid-structure interaction on connection forces in bridges due to tsunami loads. In Proceedings of the 30th US-Japan Bridge Engineering Workshop, Washington, DC, USA, 21–23 October 2014; pp. 21–23.
40. Choi, S.; Lee, K.; Gudmestad, O.T. The effect of dynamic amplification due to a structure’s vibration on breaking wave impact. *Ocean. Eng.* **2015**, *96*, 8–20. [[CrossRef](#)]
41. Istrati, D.; Buckle, I.; Lomonaco, P.; Yim, S.; Itani, A. Large-scale experiments of tsunami impact forces on bridges: The role of fluid-structure interaction and air-venting. In Proceedings of the 26th International Ocean and Polar Engineering Conference, Rhodes, Greece, 26 June 2016.
42. Sharafati, A.; Tafarjnoruz, A.; Motta, D.; Yaseen, Z.M. Application of nature-inspired optimization algorithms to ANFIS model to predict wave-induced scour depth around pipelines. *J. Hydroinform.* **2020**, *22*, 1425–1451. [[CrossRef](#)]
43. Sharafati, A.; Tafarjnoruz, A.; Shourian, M.; Yaseen, Z.M. Simulation of the depth scouring downstream sluice gate: The validation of newly developed data-intelligent models. *J. Hydro-Environ. Res.* **2020**, *29*, 20–30. [[CrossRef](#)]
44. Sharafati, A.; Tafarjnoruz, A.; Yaseen, Z.M. New stochastic modeling strategy on the prediction enhancement of pier scour depth in cohesive bed materials. *J. Hydroinform.* **2020**, *22*, 457–472. [[CrossRef](#)]
45. Hochreiter, S.; Schmidhuber, J. Long Short-Term Memory. *Neural Comput.* **1997**, *9*, 1735–1780. [[CrossRef](#)]
46. Cho, K.; van Merriënboer, B.; Bahdanau, D.; Bengio, Y. On the Properties of Neural Machine Translation: Encoder—Decoder Approaches. Available online: <https://arxiv.org/abs/1409.1259> (accessed on 1 June 2021).
47. Cho, K.; van Merriënboer, B.; Gulcehre, C.; Bahdanau, D.; Bougares, F.; Schwenk, H.; Bengio, Y. Learning Phrase Representations Using RNN Encoder—Decoder for Statistical Machine Translation. Available online: <https://arxiv.org/abs/1406.1078> (accessed on 1 June 2021).
48. Chung, J.; Gulcehre, C.; Cho, K.; Bengio, Y. Empirical Evaluation of Gated Recurrent Neural Networks on Sequence Modeling. Available online: <https://arxiv.org/abs/1412.3555> (accessed on 1 June 2021).
49. Srivastava, N.; Hinton, G.; Krizhevsky, A.; Sutskever, I.; Salakhutdinov, R. Dropout: A Simple Way to Prevent Neural Networks from Overfitting. *J. Mach. Learn. Res.* **2014**, *15*, 1929–1958.